Hindawi
Advances in Civil Engineering
Volume 2019, Article ID 3587982, 9 pages
https://doi.org/10.1155/2019/3587982

Research Article

Shear Storage Capacity of Vertical Stiffener Joints between Concrete-Filled Double Steel Tubular Columns and Steel Beams

Zhijun Zhou,[1] **Yufen Zhang**,[2] **Miao Wang**,[3] **and Krushar Demoha**[4]

[1]*School of Highway, Chang'an University, Xi'an 710064, Shaanxi Province, China*
[2]*School of Civil and Transportation Engineering, Hebei University of Technology, Tianjin 300401, China*
[3]*School of Civil Engineering, North China University of Technology, Beijing 100144, China*
[4]*Department of Mechanical Engineering, University of Auckland, Auckland, New Zealand*

Correspondence should be addressed to Yufen Zhang; yufenzh@gmail.com

Received 18 October 2018; Revised 27 November 2018; Accepted 26 December 2018; Published 3 February 2019

Academic Editor: Chiara Bedon

Based on the low cyclic loading test results of vertical stiffener joints between concrete-filled double steel tubular (CFDST) columns and steel beams, the shear transfer mechanism and shear resistance were analyzed in this paper. A conceptual model formulated was presented in terms of equilibrium and stress-strain relationships. The results calculated by the theoretical model and the available experimental data were compared, and then one new concept of shear storage coefficient was proposed for the determination of the shear storage capacity of the joint, which quantitatively explained the ductility failure progression of the joint specimens in the seismic performance test. It was concluded that the vertical stiffener joint had sufficient shear resistance, which met the seismic design principle of strong shear and weak bending. Results show that the ribbed joints have greater shear resistance than unribbed ones; lengthening the overhang of the vertical stiffener can both increase shear resistance and shear storage capacity of the joint; axial compression ratio can reduce the shear storage capacity. The paper also suggests that the joint design should ensure enough safety storage of shear resistance to improve the seismic performance.

1. Introduction

With the development of concrete-filled steel tubular (CFST) column, concrete-filled double steel tubular (CFDST) column emerged in the form of circular internally and square externally, fully filled with concrete. CFDST column can make full use of circular steel tube for its good confinement performance and square steel tube for its good ductility advantages, so the new type of column can be applied to high-rise buildings and bridge engineering [1–3]. CFDST column has been firstly applied in the construction of city hall in Wuppertal, Germany. The vertical stiffener joint between a CFDST column and an H-type beam has been verified that it has the good hysteretic behavior, bearing capacity, and ductility [4–6], but the shear behavior of the joint core has not been studied including the shear resistance. It is well known that strength calculation mainly includes bending strength and shear strength in joint design. To ensure a proper failure progression and ductility, the joint panel zone should typically be stronger than the neighboring beam and column. So, many calculation procedures for joint shear strength have been proposed. Koester [7] conducted a series of experiments on the panel zone shear strength of rectangular steel girder-to-CFST composite connections. Various shear strength for CFST joint panels has been analyzed to date [8–11]. And a simplified trilinear model to predict the shear strength versus the shear deformation response in panel zone was presented for vertical stiffener connections between L-shaped columns composed of concrete-filled steel tubes and steel beams [12]. The superposition method was also applied to estimate the beam-column joint shear strength [13–18], and the applicability and accuracy of the strength superposition method for the estimation of joint shear strength were verified explicitly. However, these studies have been limited in scope to ordinary CFST or composite concrete structures. The vertical stiffener joint of CFDST structure has very different configurations, which provide different shear components.

The shear failure of beam-column joint may cause the immediate collapse of a building, and strengthening such joints can have a significant influence upon the earthquake resistance of structures. Therefore, it is necessary to develop an effective rehabilitation strategy to strengthen such joints in order to avoid or delay their shear failure. According to the principle of structure design "strong shear and weak bending," shear strength becomes the control condition of the strength calculation. When shear strength calculation was not estimated accurately, the structure would lead to the lack of shear capacity even the shear failure [19–23], so shear storage capacity was analyzed in this paper based on the low cyclic loading test results of vertical stiffener joints between CFDST columns and steel beams. A conceptual model is presented for assessing the cracked vertical stiffener joints with shear failure. The model is entirely formulated in terms of equilibrium and stress-strain relationships and can be used to assess the shear capacity of a series of components including steel tubes, vertical stiffener, anchorage web, and joint core concrete. The calculated results were compared to the experimental ones at the state of both yielding and damage. Then, one new concept of shear storage coefficient was proposed for the determination of the joint's shear storage capacity. In order to better evaluate the seismic design principles of strong joints, the joint's safety reserve of shear capacity was quantitatively explained to ensure proper failure progression and ductility, which can provide reference for engineering design of CFDST structure.

2. The Shear Model and Force Transfer Mechanism

Vertical stiffener joints were tested by quasistatic cyclic loading at the both ends of the steel beam [6], i.e., the fixed vertical force N was applied on the column top, and two 500 kN MTS servo actuators were placed at east and west beam ends to achieve the reciprocating load by pushing and pulling at the same time. The joint specimens were intended to simulate the connection between an interior column and the two adjacent steel beams in a frame structure. Table 1 lists the details of the six specimens tested in this investigation, where l_E is the overhang length of vertical stiffener; n is the axial compressive force ratio; and two kinds of configuration of anchorage webs are unribbed and ribbed. The outer steel tube is square with the section type of $B \times t$, and the inner steel tube is circular with the section type of $\Phi 2r_i \times t_i$ as shown in Table 1. The section of H-shaped steel beam is $244 \times 175 \times 7 \times 11\ \text{mm}^4$.

Force diagram in panel zone is shown in Figure 1, where V_j represents the experimental shear force in panel zone; P is the actual load value on the beam end; H_b and H_c are the height of steel beam and column, respectively; L_b is the distance from the beam end to the surface of CFDST column; and H is the distance from the top to the bottom hinge of the column. According to the equilibrium condition, the shear force in the panel zone can be determined according to the load of the beam end in the actual experiment.

$$V_j = \frac{2PL_b}{H_b - t_b} - V_c = \frac{2PL_b}{H_b - t_b} - \frac{PL}{H}, \quad (1)$$

where V_c represents the horizontal reactive force at the column end when the beam end force is P and t_b represents the thickness of the steel beam flange.

In this joint system, anchorage web, vertical stiffeners, and horizontal end plate play the main force-transferring role. The transverse profile of the vertical stiffener joint is shown in Figure 2(a). Anchorage web is groove-welded vertically on the inner steel tube, going outside the outer steel tube, and then it connects with the steel beam web by bolts. Meanwhile vertical stiffener is groove-welded on the column surface, and its overhangs weld with the end plate at right angles. In order to solve the stress concentration problem, the radius-cut section is used for the end plate. The other side of end plate as wide as the beam is butt welded to the beam flange. In addition, the application of anchorage web embedded in the concrete between inner tube and outer tube can improve work ability and globality of the joint. And the embedded anchorage web is higher than the steel beam, so anchorage web can be chosen as two types including unribbed and ribbed joints as shown in the longitudinal profile in Figure 2(b).

The compressive strength of the concrete f_{cu} is 59.5 MPa. The material properties of the steel plates obtained through the standard material test method are given in Table 2. The steel of anchorage plate and vertical stiffener is the same steel as the square tube. The bolts were tightened with a special torque wrench according to design requirements, and the friction-type high-strength bolt M20 belongs to the level 10.9. According to the suggestion of ATC-24 [24], a displacement control with three cycles at each displacement amplitude was used after the specimen yielded. The cantilever-displacement increments between each cycle were 3 mm one time before yielding and 6 mm three times after yielding until failure occurred.

The main function of the vertical stiffener is to protect the outer steel tube web from shearing. On the other hand, together with the horizontal end plates, vertical stiffeners can transmit tension or compression of the steel beam flange, so the vertical stiffeners can bear shear force from the panel zone and horizontal pulling or pushing force from beam flanges. The anchorage web is mainly subjected to shearing force of the beam web, and the ribs can help transmit part of the pulling force from beam flanges to the joint core. The force-transferring path of the vertical stiffener joint is basically included: (1) horizontal shear force of column end is transferred to vertical stiffeners and outer steel tube by welds and then to joint core concrete; (2) vertical shear force of beam end is transferred to vertical stiffeners and anchorage webs and then to the panel zone. The calculation formula in the AIJ specification [25] proposed by the Architectural Institute of Japan takes into account the shear strength of both the steel tube cross section and the core concrete cross section. So, the shear model of the vertical stiffener joints is composed as a series of components. The shear capacity in panel zone includes the contributions from steel tubes, the vertical stiffeners, anchorage webs, and the joint core concrete. Among them, the core concrete contributes the shear capacity in the way of plane shearing and pressure lever

Table 1: Summary of the joint specimens and analysis results.

Specimens	$B \times t$ (mm^2)	$\Phi 2r_i \times t_i$ (mm^2)	l_E (mm)	n	Anchorage web	V_{yE} (kN)	V_{uE} (kN)	V_{yC} (kN)	V_{uC} (kN)	R_y	R_u
SBJ1-1	250 × 8	Φ133 × 6	80	0.23	Unribbed	1248.9	1703.9	2433.3	4070.9	1.95	2.39
SBJ1-2	250 × 8	Φ133 × 6	120	0.23	Unribbed	1373.6	1774.2	2722.9	4544.6	1.98	2.56
SBJ2-1	250 × 8	Φ133 × 6	80	0.23	Ribbed	1392.4	1959.5	2974.4	4841.8	2.14	2.47
SBJ2-2	250 × 8	Φ133 × 6	120	0.23	Ribbed	1548.3	2126.1	3264.0	5315.5	2.11	2.50
SBJ3-1	250 × 8	Φ133 × 6	80	0.40	Unribbed	1326.7	1669.5	2433.3	4070.9	1.83	2.44
SBJ3-2	250 × 5	Φ133 × 6	80	0.23	Ribbed	1325.5	1856.6	2830.2	4544.2	2.14	2.45

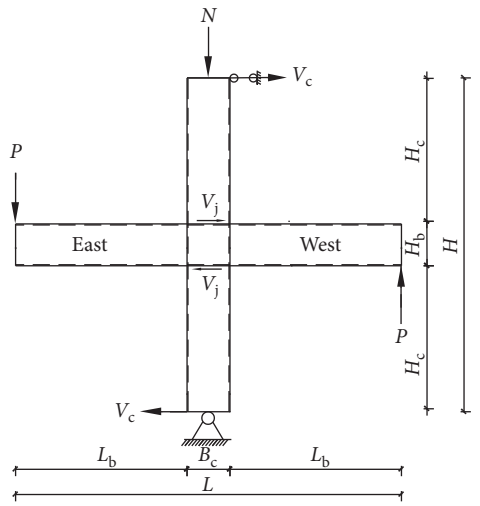

Figure 1: Force diagram in panel zone.

model, respectively. Shear capacity of each component can be calculated using different stress states based on the different deformation mechanism, and finally the ultimate shear capacity of the joint will be obtained on the principle of limit equilibrium superposition.

3. Calculation of the Theoretical Shear Resistance

3.1. Basic Assumptions. For the double steel tubes and core concrete, the effect of axial compressive stress is considered to calculate the shear capacity, while for the force-transmitting members' vertical stiffeners and anchorage webs, pure shear stress state is used without considering the effect of axial stress since they are considered as main connecting part to the beam-column connections. In order to simplify the calculation and analysis, the following basic assumptions are also introduced:

(1) There is no relative slip between steel tubes and concrete, and the axial deformation is consistent

(2) After the steel tube has yielded, the cross-sectional shape does not change, and bending deformation and local buckling of inner and outer steel tubes are ignored [26]

(3) Shear force transferring of vertical stiffener joints is through vertical stiffener and anchorage web to the outer square and inner circular steel tubes, and concrete baroclinic force transmission mode [20] is considered because there is no inner diaphragm

3.2. Outer Square Steel Tube. The circumferential tensile stress of the steel tube wall has a weakening effect on the shear capacity of the joint, so it should be considered into the calculation of the shear capacity. As the confinement of square steel tube on the concrete is not uniform, concrete-filled square tubular column can be equivalent to concrete-filled circular tube column according to the principle of equal area [27]. The shear force-shear deformation skeleton curve of outer steel tube webs is taken as trilinear model of shear [28, 29] shown in Figure 3, where V_{oy}, V_{ou}, respectively, represent the yield and ultimate shear stress of the outer steel tube web.

Figure 4 is the stress state of the outer steel tube web, where σ_{oz} is the compressive stress produced by the vertical steel tube web under the action of vertical axial compression, $\sigma_{o\theta}$ is the lateral tensile stress of the outer steel tube web, τ_o stands for the shear stress of the outer steel tube. In the following subscripts, the subscripts s and c represent steel and concrete, respectively; subscripts i and o represent inner and outer steel tube, respectively; and subscripts z, r, and θ represent longitudinal, radial, and circumferential directions, respectively. It can be seen from Figure 4 that the stress state of outer steel tube web can be expressed as $\sigma_x = \sigma_{o\theta}, \sigma_y = \sigma_{oz}, \tau_{xy} = \tau_o$, so the principal stresses of the outer steel tube are

$$\sigma_1 = \frac{\sigma_{oz} + \sigma_{o\theta}}{2} + \sqrt{\left(\frac{\sigma_{oz} - \sigma_{o\theta}}{2}\right)^2 + \tau_o^2},$$

$$\sigma_2 = 0, \tag{2}$$

$$\sigma_3 = \frac{\sigma_{oz} + \sigma_{o\theta}}{2} - \sqrt{\left(\frac{\sigma_{oz} - \sigma_{o\theta}}{2}\right)^2 + \tau_o^2}.$$

According to von Mises yield criterion, the yield stress of the outer steel tube is

$$f_{oy} = \sqrt{\frac{\left[(\sigma_1 - \sigma_2)^2 + (\sigma_2 - \sigma_3)^2 + (\sigma_3 - \sigma_1)^2\right]}{2}}, \tag{3}$$

where f_{oy} is the yield strength of the outer steel tube web. By substituting equation (2) into equation (3), we have

$$f_{oy} = \sqrt{\sigma_{oz}^2 + \sigma_{o\theta}^2 - \sigma_{oo}\sigma_{o\theta} + 3\tau_o^2}. \tag{4}$$

So, the shear stress of the outer steel tube under axial compression is

$$\tau_{oy} = \frac{1}{\sqrt{3}} \sqrt{f_{oy}^2 - \sigma_{oz}^2 - \sigma_{o\theta}^2 + \sigma_{oz}\sigma_{o\theta}}. \tag{5}$$

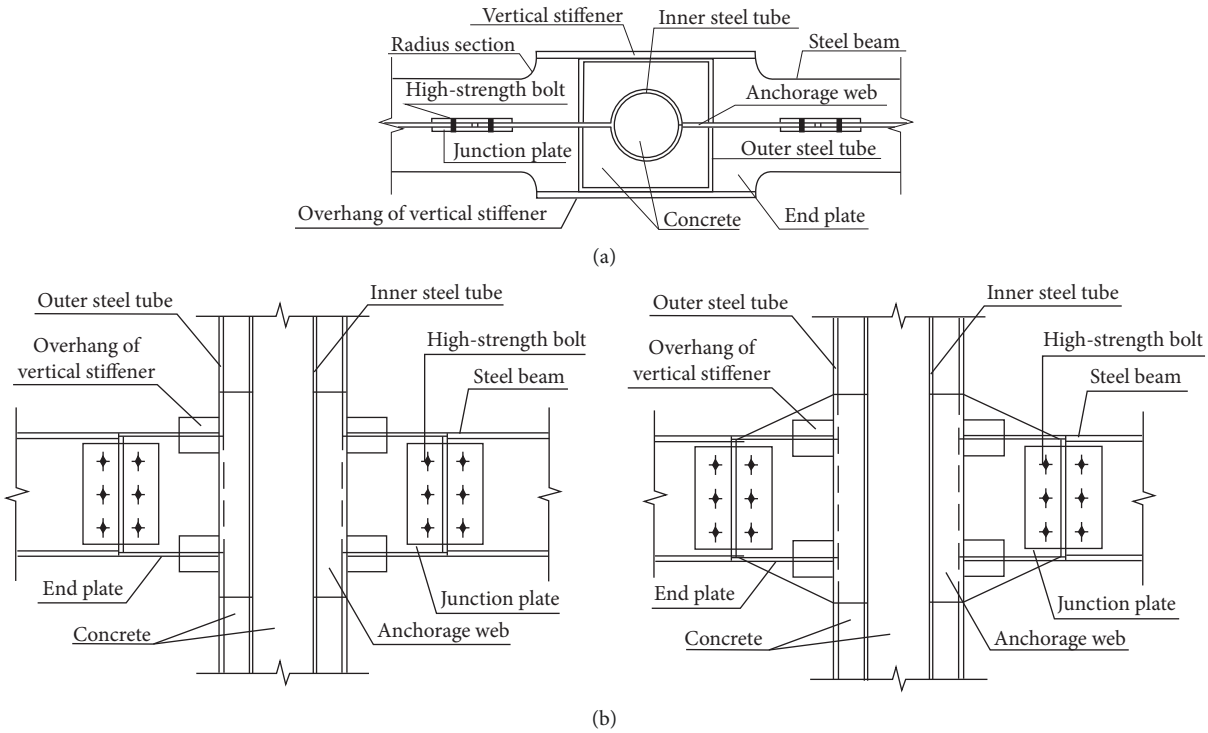

Figure 2: Details of vertical stiffener joints. (a) Transverse profile. (b) Longitudinal profile.

Table 2: Material properties of the steel.

Steel material	Square tube	Circle tube	End plate	Beam flange	Beam web
Average thickness (mm)	7.6	6.4	11.5	10.6	6.6
Yield strength (MPa)	338.12	323.08	272.61	272.41	291.00
Ultimate strength (MPa)	481.70	491.39	445.86	447.40	457.23
Elastic modulus (10^5 MPa)	2.257	2.152	2.132	2.213	2.157

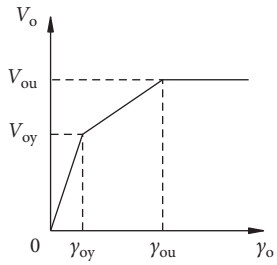

Figure 3: Trilinear shear force-deformation model.

Then, the yield shear resistance of the outer steel tube web is

$$V_{oy} = A_o \tau_{oy} = \frac{A_o}{\sqrt{3}} \sqrt{f_{oy}^2 - \sigma_{oz}^2 - \sigma_{o\theta}^2 + \sigma_{oz}\sigma_{o\theta}}, \quad (6)$$

where A_o represents the cross-sectional area of outer steel tube and V_{oy} represents the yield shear resistance of outer steel tube. The ultimate shear resistance of outer steel tube based on the trilinear shear model is

$$V_{ou} = \frac{A_o}{\sqrt{3}} \sqrt{f_{ou}^2 - \sigma_{oz}^2 - \sigma_{o\theta}^2 + \sigma_{oz}\sigma_{o\theta}}. \quad (7)$$

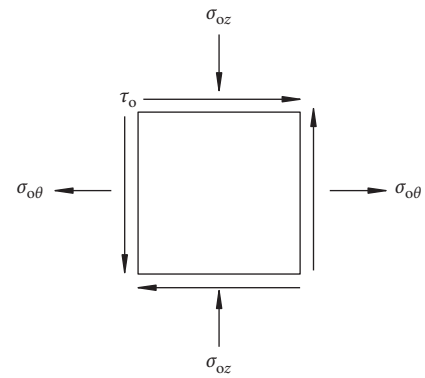

Figure 4: Stress state of steel plate of outer steel tube.

3.3. Inner Circular Steel Tube. Similar with the outer steel tube, the inner steel tube has the same stress state as shown in Figure 4. Its shear stress is $\tau_{iy} = (1/\sqrt{3})\sqrt{f_{iy}^2 - \sigma_{iz}^2 - \sigma_{i\theta}^2 + \sigma_{iz}\sigma_{i\theta}}$; the yield shear resistance of the inner circular steel tube is

$$V_{iy} = A_i \tau_{iy} = \frac{A_i}{\sqrt{3}} \sqrt{f_{iy}^2 - \sigma_{iz}^2 - \sigma_{i\theta}^2 + \sigma_{iz}\sigma_{i\theta}}. \quad (8)$$

Then, the ultimate shear resistance of the inner circular steel tube is described as

$$V_{iu} = \frac{A_i}{\sqrt{3}} \sqrt{f_{iu}^2 - \sigma_{iz}^2 - \sigma_{i\theta}^2 + \sigma_{iz}\sigma_{i\theta}}, \quad (9)$$

where V_{iy} denotes the yield shear resistance of the inner circular steel tube and V_{iu} denotes the ultimate shear resistance of the inner circular steel tube. The shearing area of the inner circular steel tube is A_i. In literature [30], $A_i = \pi R \times t_i$ was obtained when shear strength was analyzed by the method of elastic mechanics, where R is the radius of the inner circular tube. In this paper, the inner round steel tube is wrapped in the concrete of the CFDST column, so the shear capacity has been improved absolutely. Taking into account the simplified method of material mechanics, the projection area of round tube diameter is taken as shearing area, that is, $A_i = 2\ d \times t_i = 4R \times t_i$, where d represents the diameter of the inner circular pipe and t_i represents the wall thickness of the inner circular steel tube.

3.4. Vertical Stiffeners. The vertical stiffeners are taken in pure shear stress state without considering the effect of axial stress since they are considered as main connecting part to the beam-column connections. Stress state of vertical stiffeners is $\sigma_x = 0, \sigma_y = 0,\ \tau_{xy} = -\tau_v$; therefore, the principal stresses are $\sigma_1 = \tau_v\ ; \sigma_2 = 0;\ \sigma_3 = -\tau_v$. According to von Mises yield criterion, the shear stress of the vertical stiffeners is obtained: $\tau_{vy} = f_{vy}/\sqrt{3}$, where f_{vy} is the yield strength of the vertical stiffeners. So, the yield shear resistance and the ultimate shear resistance of the vertical stiffener are listed, respectively, as follows:

$$V_{vy} = A_v \tau_{vy} = \frac{f_{vy} A_v}{\sqrt{3}}, \quad (10)$$

$$V_{vu} = \frac{f_{vu} A_v}{\sqrt{3}}, \quad (11)$$

where A_v is the horizontal cross-sectional area of the whole vertical stiffeners, f_{vu} is the ultimate strength of the vertical stiffeners, V_{vy} represents the yield shear resistance of the vertical stiffener, and V_{vu} represents the ultimate shear resistance of the vertical stiffener.

3.5. Anchorage Web. An anchored web is welded to the inner steel tube, and its extended part out of the outer steel tube is connected to the steel beam web. The yield shear stress of the anchored web is known from the foregoing conclusions as $\tau_{ay} = f_{ay}/\sqrt{3}$, where f_{ay} is the yield strength of the anchorage web, so yield shear resistance and ultimate shear resistance of the anchored web are, respectively, expressed as follows:

$$V_{ay} = A_a \tau_{ay} = \frac{f_{ay} A_a}{\sqrt{3}}, \quad (12)$$

$$V_{au} = \frac{f_{au} A_a}{\sqrt{3}}, \quad (13)$$

where A_a denotes shearing area of the anchorage web. The anchorage web has two types including ribbed and unribbed ones. For the unribbed anchorage web, shearing area is calculated as its horizontal cross-sectional area between inner and outer steel tubes, while for the ribbed anchorage web, shearing area is calculated as its full horizontal cross-sectional area. f_{au} is ultimate strength of the anchorage web. V_{ay} is yield shear resistance of the anchorage web, and V_{ay} is ultimate shear resistance of the anchorage web.

3.6. Outer and Inner Concrete. The inner and outer concrete are constrained by steel tubes, and due to the presence of axial pressure, the core concrete is under three-dimensional compression state, so the shear strength of concrete can maintain a constant value without a decline when it reaches the ultimate shear strength. Therefore, the shear stress-strain curve of core concrete is simplified as the ascending and horizontal segments as shown in Figure 5.

The shear strength and shear deformation of concrete are studied in 1992 [31]. According to those experimental results, the ascending curve of shear stress-shear strain is obtained as follows:

$$\begin{aligned} y &= 0.8x^4 - 1.7x^3 + 1.9x, \\ x &= \frac{\gamma}{\gamma_p}, \\ y &= \frac{\tau}{\tau_p}, \end{aligned} \quad (14)$$

where γ_p and τ_p represent the peak shear strain and stress, respectively, $\tau_p = 0.42 f_{cu}^{0.55}$ and $\gamma_p = (176.80 + 83.56\tau_p) \times 10^{-6}$; then, the shear resistance of inner and outer concrete is considered as

$$V_c = \tau (A_{co} + A_{ci}), \quad (15)$$

where A_{co} and A_{ci}, respectively, represent the cross-sectional area of outer and inner concrete.

4. Test Results and Shear Storage Capacity

Figure 6 reveals beam end load (P) versus displacement (Δ) envelope curves of the six joint specimens on west (W) and east (E) beam ends. For the convenience of presentation, the loading force is considered as positive when the actuators push and negative when the actuators pull, while the push displacement of the west end is considered as

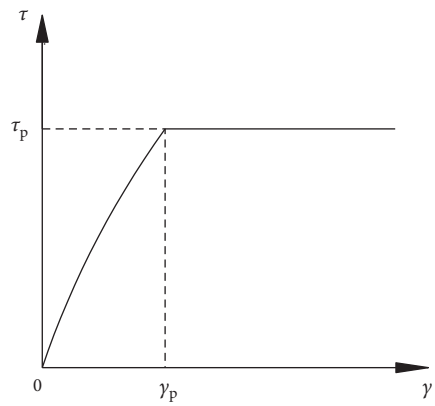

Figure 5: Shear stress-strain curve of the core concrete.

positive and the push displacement of the east end as negative. The yield load P_y of joints is determined according to Figure 7. The yield load and ultimate load in the test are taken as the average value of push and pull force on both west and east beam ends. Then, the corresponding magnitude of shear forces in the test can be obtained by equation (1). The shear force in the panel zone at the state of yield load and ultimate load in the test is listed in Table 1, where V_{yE} represents the shear force corresponding to the average yield load of east and west beams and V_{uE} represents the shear force corresponding to the average ultimate load of east and west beams.

The theoretical shear resistance of the vertical stiffener joints is calculated by the principle of superposition according to the limit equilibrium theory. Based on the aforementioned equations of the shear capacity of the joint components, the calculated shear capacity is listed in Table 1. V_{yC} is the calculated theoretical yield shear resistance obtained from Equations (6), (8), (10), (12), and (15); V_{uC} is the calculated theoretical ultimate shear resistance obtained from Equations (7), (9), (11), (13), and (15). In the calculations, ribbed anchorage web and vertical stiffener plate provide a large amount contribution to the joint's shear resistance. Therefore, the ribbed joints have greater shear capacity than unribbed ones, and shear resistance improves with the increase of overhang length of vertical stiffener. By comparison of specimens SBJ2-1 and SBJ3-2, the thickness of square steel tube has a slight influence on the joint's shear capacity. It can be concluded that the force-transferring connectors including vertical stiffeners and anchorage webs play a dominant role in the shear bearing capacity of the joint.

As can be seen in Table 1, compared with the experimental data of six joint specimens in the seismic performance test, the calculated results of yield shear resistance and ultimate shear resistance are much larger than the experimental shear force corresponding to the cracked vertical stiffener joint. It indicates that the joint has enough shear storage ability to avoid the shear failure of the panel zone. The main reason is that the vertical stiffener joints in the experiment belong to the "strong column and weak beam" type, so the failure modes of the specimens are roughly the similar damage caused by the bending failure at beam ends. The plastic hinge occurred away from the curvature of the horizontal end plate in the test as shown in Figure 8. Strain measured in the test also showed the panel zone was in elastic state basically. So, the steel tubes, connectors (including anchorage web and vertical stiffeners), and core concrete worked in good mechanical performance to guarantee the strong shear capacity and stiffness, indicating that such joint design is in line with "strong shear and weak bending" principle of the seismic design.

In fact, V_{uC} is the calculated ultimate shear resistance for cracked vertical stiffener joints with shear failure, while V_{uE} is the shear force corresponding to the cracked experimental joints with bending failure, so the theoretical resistance proposed cannot be checked via full strength joints since the beam resistant bending moment is limiting the maximum shear strength. However, it indicates that the configuration of vertical stiffener joints can guarantee an effective rehabilitation strategy to strengthen such joints in order to avoid or delay their shear failure. This storage ability can be reflected by shear storage coefficient. The so-called shear storage coefficient is the ratio between the theoretical shear resistance and the actual shear force in experiments, which is described as

$$R_y = \frac{V_{yC}}{V_{yE}}, \tag{16}$$

$$R_u = \frac{V_{uC}}{V_{uE}}, \tag{17}$$

where R_y is the shear storage coefficient at the yield state and R_u is the shear storage coefficient at the ultimate load state. In fact, the shear storage coefficient in equations (16) and (17) is not a new concept of shear reserve. In the verification of seismic ability in some structure, the ratio of shear capacity and the actual shear force in earthquake must be greater than 1 [32, 33]. The paper puts forward this ratio for the vertical stiffener joint to quantify its shear safety reserves. Shear storage coefficient of the joint mainly takes the quantitative relationship between its shear bearing capacity and shear failure into account, so as to better evaluate the seismic design principle of strong joints and provide reference for the improvement of joint seismic design codes. The shear storage coefficient determines the safe storage capacity to ensure a proper failure progression and ductility of these joints, and increasing the shear storage coefficient can improve the seismic performance of the joint as well. The calculations of shear storage coefficient are shown in Table 1, where R_y is obtained as 2.02 at average and R_u is 2.47. The shear storage coefficient R_y and R_u of SBJ3-1 with the higher axial compression ratio is the smallest as shown in Table 1, so axial compression ratio can reduce the shear storage capacity of the joint. By comparison of specimens SBJ1-1, SBJ1-2, SBJ2-1, and SBJ2-2, it can also be concluded that lengthening the overhang of the vertical stiffener can increase the joint's shear storage capacity, while the influence of ribs is not evident.

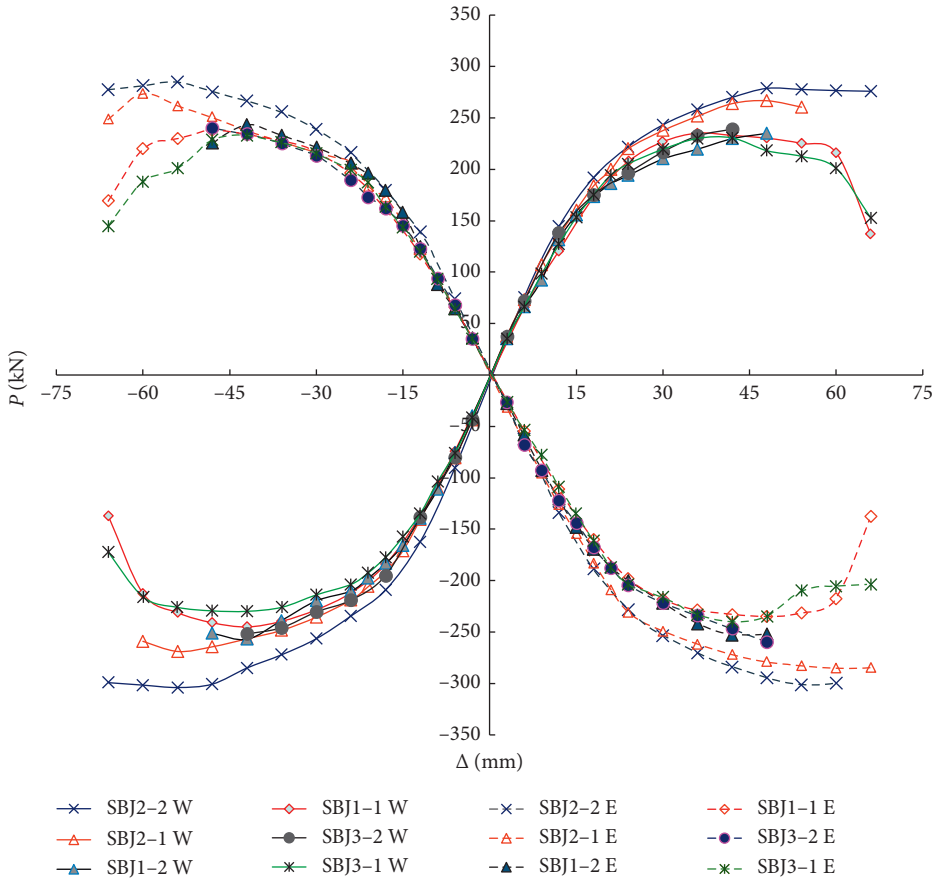

Figure 6: Skeleton curves of P-Δ on beam ends.

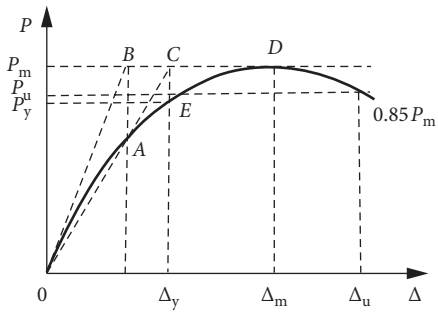

Figure 7: Determination for the yield load in test.

Figure 8: The failure mode in the test.

5. Conclusions

On the basis of the low cyclic loading test results of vertical stiffener joints between concrete-filled double steel tubular (CFDST) columns and steel beams, the shear storage capacity was analyzed in this paper. A conceptual model was presented for assessing the cracked vertical stiffener joint. The shear performance and force transfer mechanism were reasonably assumed. The model was entirely formulated in terms of equilibrium and stress-strain relationships and could be used to effectively assess the shear capacity of a series of components including steel tubes, vertical stiffener, anchorage web, and joint core concrete. The shear capacity equation of the joints provided a simplified calculation method and corresponding reference for the engineering design of CFDST structure.

The yield and ultimate shear resistance of the vertical stiffener joints of CFDST were calculated and compared with the experimental results, and one new index of shear storage coefficient was put forward in order to quantitatively explain the safe reserve of ductile failure. Shear storage coefficient determined the safe storage capacity of the joint to avoid its shear failure mode, and improving the reserve coefficient can ensure proper failure progression and ductility. The results show that the ribbed joints have greater shear resistance than

unribbed ones, while the influence on shear storage capacity is not evident; lengthening the overhang of the vertical stiffener can increase both the shear resistance and joint's shear storage capacity; axial compression ratio can reduce the joint's shear storage capacity. Therefore, the vertical stiffener joint has enough safety storage to meet the seismic design principle of "strong shear and weak bending."

Data Availability

The data used to support the findings of this study are available from the corresponding author upon request.

Conflicts of Interest

The authors declare that there are no conflicts of interest regarding the publication of this article.

Acknowledgments

The authors would like to acknowledge the support provided by the Chinese National Science Foundation (grant no. 51478004). The financial support from Hebei University of Technology is also appreciated.

References

[1] S. H. Cai, *Modern Steel Tube Concrete Structure*, People's Communications Press, Beijing, China, 2003, in Chinese.

[2] Y.-F. Zhang and Z.-Q. Zhang, "Study on equivalent confinement coefficient of composite CFST column based on unified theory," *Mechanics of Advanced Materials and Structures*, vol. 23, no. 1, pp. 22–27, 2015.

[3] G. Du, A. Andjelic, Z. Li, Z. Lei, and X. Bie, "Residual axial bearing capacity of concrete-filled circular steel tubular columns (CFCSTCs) after transverse impact," *Applied Sciences*, vol. 8, no. 5, p. 793, 2018.

[4] D. F. Zhang, J. H. Zhao, Y. F. Zhang et al., "Finite element analysis of seismic performance of composite concrete-filled steel tube column-steel beam connection," *World Earthquake Engineering*, vol. 29, no. 1, pp. 49–59, 2013, in Chinese.

[5] Y. F. Zhang and Z. Q. Zhang, "Connection design of concrete-filled twin steel tubes column," in *Proceedings of 2014 Structural and Civil Engineering Workshop (SCEW 2014)*, pp. 365–370, Tokyo, Japan, November 2014.

[6] Y. F. Zhang and D. F. Zhang, "Experimental study on the seismic behaviour of the connection between concrete-filled twin steel tubes column and steel beam," *European Journal of Environmental and Civil Engineering*, vol. 19, no. 3, pp. 347–365, 2014.

[7] B. D. Koester, *"Panel zone behavior of moment connections between rectangular concrete-filled steel tubes and wide flange beams,"* Ph.D. dissertation, University of Texas, Austin, Texas, USA, 2000.

[8] L. Jian, "Shear strength of connections between concrete filled steel tubes and beams," *Applied Mechanics and Materials*, vol. 351-352, pp. 75–79, 2013.

[9] L. Kang, R. T. Leon, X. Lu, and X. L. Lu, "Shear strength analyses of internal diaphragm connections to CFT columns," *Steel and Composite Structures*, vol. 18, no. 5, pp. 1083–1101, 2015.

[10] G. Parra-Montesinos and J. K. Wight, "Modeling shear behavior of hybrid RCS beam-column connections," *Journal of Structural Engineering*, vol. 127, no. 1, pp. 3–11, 2001.

[11] M. H. Jones and Y. C. Wang, "Experimental studies and numerical analysis of the shear behavior of fin plates to tubular columns at ambient and elevated temperatures," *Steel and Composite Structures*, vol. 8, no. 3, pp. 179–200, 2008.

[12] W. Zhang, Z. Chen, Q. Xiong, and T. Zhou, "Calculation method of shear strength of vertical stiffener connections to L-CFST columns," *Advances in Structural Engineering*, vol. 21, no. 6, pp. 795–808, 2017.

[13] A. Soler, A. Barroso, and V. Mantič, "Failure initiation criterion in bonded joints with composites based on singularity parameters and practical procedure for design purposes," *Composite Interfaces*, vol. 22, no. 8, pp. 743–755, 2015.

[14] H. París, S. Z. Li, and Z. Li, "Shear behavior of composite frame inner joints of SRRC column-steel beam subjected to cyclic loading," *Steel and Composite Structures*, vol. 27, no. 4, pp. 495–508, 2018.

[15] A. P. Ramos, V. J. G. Lúcio, and D. M. V. Faria, "The effect of the vertical component of prestress forces on the punching strength of flat slabs," *Engineering Structures*, vol. 76, pp. 90–98, 2014.

[16] A. Oinonen and G. Marquis, "Shear damage simulation of adhesive reinforced bolted lap-connection interfaces," *Engineering Fracture Mechanics*, vol. 109, pp. 341–352, 2013.

[17] C.-C. Chen, B. Suswanto, and Y.-J. Lin, "Behavior and strength of steel reinforced concrete beam-column joints with single-side force inputs," *Journal of Constructional Steel Research*, vol. 65, pp. 1569–1581, 2009.

[18] C.-C. Chen and K.-T. Lin, "Behavior and strength of steel reinforced concrete beam-column joints with two-side force inputs," *Journal of Constructional Steel Research*, vol. 65, pp. 641–649, 2009.

[19] T. Wu, X. Liu, D. Y. Li, G. H. Xing, and B. Q. Liu, "Study on the shear strength of interior joints of reinforced concrete frames based on the Bayesian theory," *Engineering Mechanics*, vol. 32, no. 3, pp. 167–174, 2015.

[20] J. G. Nie and G. G. Xu, "Shear stress analysis of concrete filled square steel tubular joints," *Journal of Tsinghua University*, vol. 49, no. 6, pp. 782–786, 2009, in Chinese.

[21] C. Amadio, C. Bedon, M. Fasan, and M. R. Pecce, "Refined numerical modelling for the structural assessment of steel-concrete composite beam-to-column joints under seismic loads," *Engineering Structures*, vol. 138, no. 5, pp. 394–409, 2017.

[22] L. Xiao, X. Z. Li, and Z. G. John Ma, "Behavior of perforated shear connectors in steel-concrete composite joints of hybrid bridges," *Journal of Bridge Engineering*, vol. 22, no. 4, article 04016135, 2017.

[23] N. E. Shanmugam, C. H. Yu, J. Y. R. Liew, and T. H. Teo, "Modelling of steel-concrete composite joints," *Journal of Constructional Steel Research*, vol. 46, no. 1-3, pp. 247–249, 1998.

[24] ATC-24, *Guidelines for Cyclic Seismic Testing of Components of Steel Structures*, Applied Technology Council, Redwood City, CA, USA, 1992.

[25] Architectural Institute of Japan (AIJ), *AIJ Standard for Structural Calculation of Steel Reinforced Concrete Structures*, AIJ, Tokyo, Japan, 1987.

[26] M. Pop, O. Corbu, and P. Pernes, "Steel-concrete materials performance in composite joints configuration," *IOP Conference Series: Materials Science and Engineering*, vol. 209, no. 1, article 012103, 2017.

[27] Y. F. Zhang, J. H. Zhao, and W. F. Yuan, "Study on compressive bearing capacity of concrete filled square steel tube column reinforced by circular steel tube inside," *Journal of Civil Engineering and Management*, vol. 19, no. 6, pp. 787–795, 2013.

[28] I. Nishiyama, T. Fujimoto, T. Fukumoto, and K. Yoshioka, "Inelastic force-deformation response of joint shear panels in beam-column moment connections to concrete-filled tubes," *Journal of Structural Engineering*, vol. 130, no. 2, pp. 244–252, 2004.

[29] T. Fukumoto and K. Morita, "Elastoplastic behavior of panel zone in steel beam-to-concrete filled steel tube column (CFT) column connections," in *Proceedings of the 6th ASCCS Conference Vol. 1: Composite and Hybrid Structures, Los Angeles*, pp. 565–572, CA, USA, March 2000.

[30] D. X. Zhang and S. M. Zhang, "Shear strength of concrete filled steel tubular column and beam joint," *Journal of Harbin University of Civil Engineering and Architecture*, vol. 34, no. 3, pp. 35–39, 2001, in Chinese.

[31] Q. Zhang and Z. H. Guo, "Study on shear strength and shear deformation of concrete," *Journal of Building Structures*, vol. 13, no. 5, pp. 17–24, 1992, in Chinese.

[32] S. C. Zhao, Y. H. Liu, J. A. Kou et al., "Preliminary research on seismic capacity reserve for ductile and brittle structures," *Journal of Southwest Jiaotong University*, vol. 44, no. 3, pp. 327–335, 2009, in Chinese.

[33] B. R. Ding, "Analysis of typical seismic damage of two categories of structures," Master's Degree Thesis, Institute of Engineering Mechanics, China Earthquake Administration, Harbin, China, 2011.